fibers

MDPI

Article

Combined Functionalization of Carbon Nanotubes (CNT) Fibers with H_2SO_4/HNO_3 and $Ca(OH)_2$ for Addition in Cementitious Matrix

Eduardo Batiston [1,2], Paulo Ricardo de Matos [2,*], Philippe Jean Paul Gleize [2], Roman Fediuk [3,*], Sergey Klyuev [4], Nikolai Vatin [5] and Maria Karelina [6]

1 Department of Civil Engineering, Community University of the Chapecó Regions, Chapeco 89809-900, Brazil; erbatiston@unochapeco.edu.br
2 Department of Civil Engineering, Federal University of Santa Catarina, Florianópolis 88040-900, Brazil; p.gleize@ufsc.br
3 Polytechnic Institute, Far Eastern Federal University, 690922 Vladivostok, Russia
4 Department of Theoretical Mechanics and Strength of Materials, Belgorod State Technological University Named after V.G. Shukhov, 308012 Belgorod, Russia; klyuyev@yandex.ru
5 Institute of Civil Engineering, Peter the Great St. Petersburg Polytechnic University, 195251 St. Petersburg, Russia; vatin@mail.ru
6 Department of Road-Building Materials, Moscow Automobile and Road Construction University, 125319 Moscow, Russia; Karelinamu@mail.ru
* Correspondence: paulorm.matos@gmail.com (P.R.d.M.); fedyuk.rs@dvfu.ru (R.F.)

Abstract: Acid treatment is commonly used to improve the dispersion of carbon nanotubes (CNT) in a cementitious matrix, but it causes undesired delay on cement hydration kinetics. This work reports a combined CNT functionalization method with H_2SO_4/HNO_3 and $Ca(OH)_2$ for addition in a cementitious matrix. Results showed that the $Ca(OH)_2$ exposure neutralized the active sites generated by acid exposure, compensating the delay in hydration. As a result, CNT exposed to H_2SO_4/HNO_3 for 9 h and further $Ca(OH)_2$ treatment led to equivalent hydration kinetics than un-treated CNT did with improved stability.

Keywords: carbon nanotube; fiber; functionalization; cementitious matrix

Citation: Batiston, E.; de Matos, P.R.; Gleize, P.J.P.; Fediuk, R.; Klyuev, S.; Vatin, N.; Karelina, M. Combined Functionalization of Carbon Nanotubes (CNT) Fibers with H_2SO_4/HNO_3 and $Ca(OH)_2$ for Addition in Cementitious Matrix. *Fibers* **2021**, *9*, 14. https://doi.org/10.3390/fib9030014

Academic Editor: Martin J. D. Clift

Received: 8 January 2021
Accepted: 1 February 2021
Published: 1 March 2021

1. Introduction

Carbon nanotubes (CNT) incorporation in cement-based materials can improve their mechanical performance by acting as bridges across cracks and voids, therefore increasing the strength and toughness of the composite [1–4]. In addition, the very high specific surface area (SSA) of CNT tends to accelerate the early hydration kinetics of cement, resulting in mechanical strength gains even at early ages [5–8]. However, properly dispersing CNT is a challenge due to its high SSA, clustering formation, and Van der Waals attractive forces [9–12].

The main methods for dispersing CNT are mechanical dispersion (e.g., high-speed ball milling) [13–16], ultrasonic dispersion [17–20], electric field induction [21–23], surface modification (also called functionalization) [1,24,25], or a combination of these methods. Among the functionalization methods, the most common is by exposing the CNT to a highly acidic environment (e.g., solution of sulfuric and nitric acid) [26–28]. In this condition, oxygen atoms from the acid can react with the carbon atoms of the defect sites and/or ends of CNT. As a consequence, some polar groups may be formed (e.g., –COH and –COOH), improving the wettability of CNT in water [29–31].

When CNTs are added to fresh cement mix, the polar groups formed by the functionalization process can bind with ions from the pore solution, delaying the cement hydration kinetics. This delay can slow down the formation of the microstructure of the cementitious matrix [4,32,33], impairing the mechanical strength of the composite at early ages [34–37].

In this context, Mendoza Reales et al. [38] evaluated the effect of a commercial dispersion of CNT on the hydration of a class G cement paste, finding that CNT addition delayed the induction period by up to 15 h, and this delay was proportional to the CNT content added. Torabian Isfahani et al. [39] produced cement pastes with 0 and 0.1 wt. % of functionalized CNT, finding that the incorporation of functionalized CNT reduced the 24-h cumulative heat by 3% compared with plain cement paste. Indirectly, Ahmed et al. [40] observed lower strength increases when functionalized CNT were added compared with un-treated CNT.

In order to prevent such undesired delay on cement hydration, this work investigated a combined functionalization of CNT with acid and calcium hydroxide for addition in cementitious matrix.

2. Materials and Methods

2.1. Materials

CNT manufactured by Cheap Tubes Inc. was used, with density of 1.7 g/cm^3, external diameter of 8–15 nm, length of 10–50 nm, and 95% purity. Scanning electron microscopy (SEM) images of CNT are shown later in Section 3.1. A Portland cement type CP I-S [41] was used for paste preparation, the characteristics of which were provided by the manufacturer, as presented in Table 1. A polycarboxylate-based superplasticizer was used to achieve proper flowability, with pH of about 6, density of 1.09 g/cm^3, and solid content of 30.5%.

Table 1. Chemical and physical characteristics of the Portland cement used.

Property	Value
Chemical composition (wt. %)	
SiO_2	20.17
Al_2O_3	4.06
Fe_2O_3	3.33
CaO	60.96
MgO	3.54
SiO_3	3.43
K_2O	1.1
Na_2O	0.09
Loss on ignition	3.05
Insoluble residue	0.27
Physical property	
Fc 1 day (MPa)	23.8
Fc 3 day (MPa)	29.2
Fc 28 day (MPa)	40.2
Density (g/cm^3)	3.11
Blaine fineness (cm^2/g)	3460

Fc: nominal compressive strength.

The pastes were prepared with distilled water, using a water/cement ratio of 0.30 by weight, with the addition of both superplasticizer and CNT in 0.1 wt. % over the cement weight. Firstly, CNTs, water, and superplasticizer were mixed and sonicated for 20 min at 55 kHz in a low energy water bath sonicator (to prevent damaging the CNTs). Then, this suspension was mechanically mixed with the cement for 3 min.

2.2. CNT Treatment

Functionalization was conducted by immersing the CNT in a solution containing one part of HNO_3 (65%) and three parts of H_2SO_4 (92%) in volume, for three different exposure times: three, six, and nine hours. The mixtures contained 100 mL of the acid solution and 10 mg of nanotubes. During the exposure, samples were kept in agitation using an ultrasonic bath. After the exposure to acid, samples were diluted in distilled water in the ratio of 100 mL of water for every 1 mL of acid + CNT solution. The solution was kept resting for 1 h, then filtered. The material retained on the filtration membrane

was washed with distilled water and filtered until the residue reached a pH of 6 ± 1. In addition, a sample of CNT exposed to 9 h of acid treatment was further immersed in an aqueous solution of calcium hydroxide ($Ca(OH)_2$) with a concentration of 1 g/L for 24 h, subsequently being washed and air-dried.

The samples were named according to the CNT treatment: CNT-0, -3, -6, and -9 respectively for zero, three, six, and nine hours of acid exposure, in addition to CNT-9-CH for the sample with coupled acid and $Ca(OH)_2$ treatment.

2.3. Testing Methods

Zeta potential was conducted using a Zetasizer Nano ZS (Malvern) equipment in pH of 2–12. Raman spectrometry was conducted in a Ínvia (Renishaw) equipment with argon laser and wavelength of 514.5 nm within the green range of the visible light spectrum. SEM was conducted using a JSM 6701F (JEOL) microscope operating at 15 kV. Isothermal calorimetry was conducted on a TAM Air (TA Instruments) calorimeter at 21 °C for up to 50 h in paste samples of about 10 g.

3. Results and Discussion

3.1. CNT Treatment

Figure 1 shows the zeta potential and sedimentation of the CNT with different treatments. Un-treated CNT had an isoelectric point at a pH of 9.5 while increasing the H_2SO_4/HNO_3 exposure time progressively decreased the pH of the isoelectric point. Consequently, CNT-9 had the highest stability among the samples (as visually confirmed in Figure 1b), with no isoelectric point and zeta potential from about −20 to −36 mV for pH of 8.5–12.0. The increase in exposure time to acid treatment progressively increases the formation of defects, i.e., active sites, as previously reported by [26,42]. In turn, subsequent $Ca(OH)_2$ neutralization (CNT-9-CH) reduced the absolute zeta potential values compared with the non-neutralized suspension (CNT-9), indicating that the rapidly ionizable active sites created by the functionalization—which generate negative charge in solution—have been reduced.

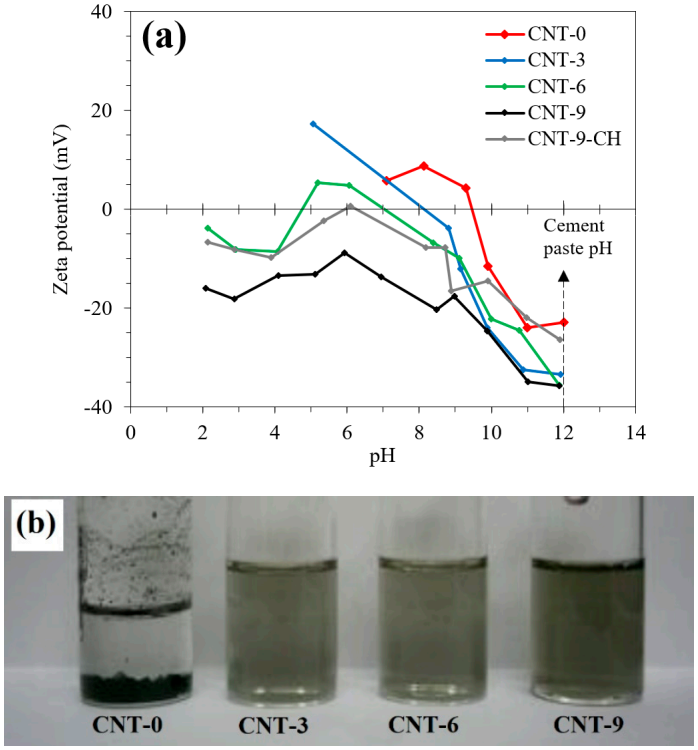

Figure 1. Zeta potential (**a**) and sedimentation (**b**) of the carbon nanotubes (CNT) with different exposure times to H_2SO_4/HNO_3 solution.

Furthermore, the pH of cement pore solution is around 12, at 25 °C [43]. For this pH, all the CNT submitted to acid treatment had zeta potential from −33 to −36 mV, while un-treated CNT had −22.8 mV, confirming that H_2SO_4/HNO_3 functionalization increased CNT stability in the pH of cement paste. The additional $Ca(OH)_2$ neutralization led to a zeta potential of −26.3 mV, partially reducing the dispersibility of CNT when compared to acid-traded CNTs, but still 15% higher than un-treated CNT.

Figure 2 shows the Raman spectra of the CNT with different exposure times to H_2SO_4/HNO_3 solution, where two bands are identified: D-bands (ID) at around 1340 cm^{-1}, which corresponds to the disorder-induced band associated with structural defects, and G-bands (IG) around 1570 cm^{-1}, associated with carbon-carbon stretching from graphite [44]. An increase in the ID/IG ratio was observed when CNTs were treated regardless of the exposure time, confirming the increase in the number of structural defects on the surface of the nanotubes [45]. Despite the increase in the number of defects with the functionalization, SEM images in Figure 3 showed that no significant changes in the overall morphology of CNT occurred, indicating that the acid treatment was not harmful to the integrity of the CNT.

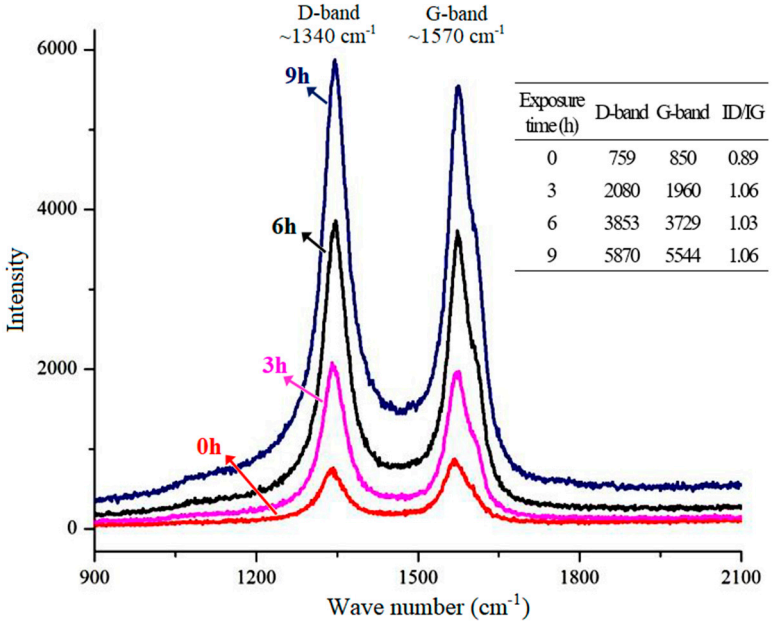

Exposure time (h)	D-band	G-band	ID/IG
0	759	850	0.89
3	2080	1960	1.06
6	3853	3729	1.03
9	5870	5544	1.06

Figure 2. Raman spectra of the CNT with different exposure times to H_2SO_4/HNO_3 solution.

3.2. Cement Hydration Kinetics

Figure 4 shows the isothermal calorimetry curves of the cement pastes, and Table 2 summarizes the testing results. The "Control" mix corresponds to a plain cement paste, i.e., without CNT addition. The incorporation of un-treated CNT (CNT-0) enhanced the early-age hydration of the cement compared with the Control mix, anticipating the occurrence of the main peak of heat release from 21.5 to 20.2 h and increasing the heat flow peak value from 2.03 to 2.18 mW/g of cement while reducing the induction period. The latter corresponds to the period of low reaction rate before the main cement reaction peak and is pointed out in Figure 4a. This behavior can be attributed to the high SSA of CNT: the incorporation of small particles provides extra surface to the nucleation and growth of the hydrated products resulting from the cement reaction, thus enhancing the early-age hydration kinetics [46–49], as reported by [5] for CNT incorporation in cement composite. In contrast, CNT functionalization delayed the cement hydration kinetics, and such delay increased as the acid exposure time increased: the main heat flow peak reduced down to 1.98 mW/g of cement and occurred up to 25.6 h for CNT-9. The polar groups created by the acid functionalization (e.g., –COH and –COOH) can bind with the $Ca(OH)_2$ formed

by cement hydration reactions [29,30]. Since the saturation of Ca^{2+} and consequent precipitation of $Ca(OH)_2$ is recognized as the trigger for the end of the induction period [35], the capture of Ca^{2+} ions by those groups can delay that saturation and consequently the overall cement reactions.

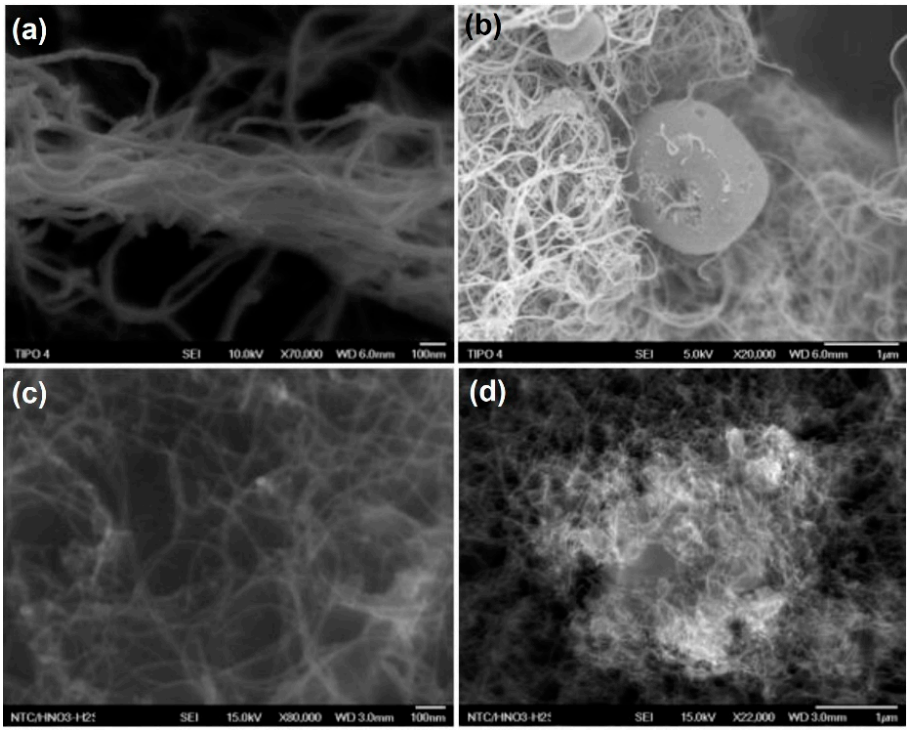

Figure 3. SEM images of the CNT: before H_2SO_4/HNO_3 exposure [×70,000 (**a**); ×20,000 (**b**)]; after H_2SO_4/HNO_3 exposure [×80,000 (**c**); ×22,000 (**d**)].

Table 2. Summary of the isothermal calorimetry.

Mix	Heat Flow Peak	
	Value (mW/g Cement)	Occurrence Time (h)
Control	2.03	21.5
CNT-0	2.18	20.2
CNT-3	2.05	23.2
CNT-6	2.03	24.8
CNT-9	1.98	25.6
CNT-9-CH	2.11	20.5

Figure 4b shows the results for the pastes containing CNT with (CNT-9-CH) and without (CNT-0 and -9) subsequent $Ca(OH)_2$ neutralization. The neutralization compensated the hydration delay caused by the acid treatment even for the highest exposure time investigated, resulting in a heat flow peak value of 2.11 mW/g of cement and occurrence time of 20.5 h for CNT-9-CH, similar to those of the CNT-0 mix (2.18 mW/g of cement and 20.2 h, respectively). This indicates that the polar groups formed in CNT bound with Ca^{2+} ions from the $Ca(OH)_2$ neutralization solution before its addition in the paste, preventing the undesired delay in the cement hydration kinetics.

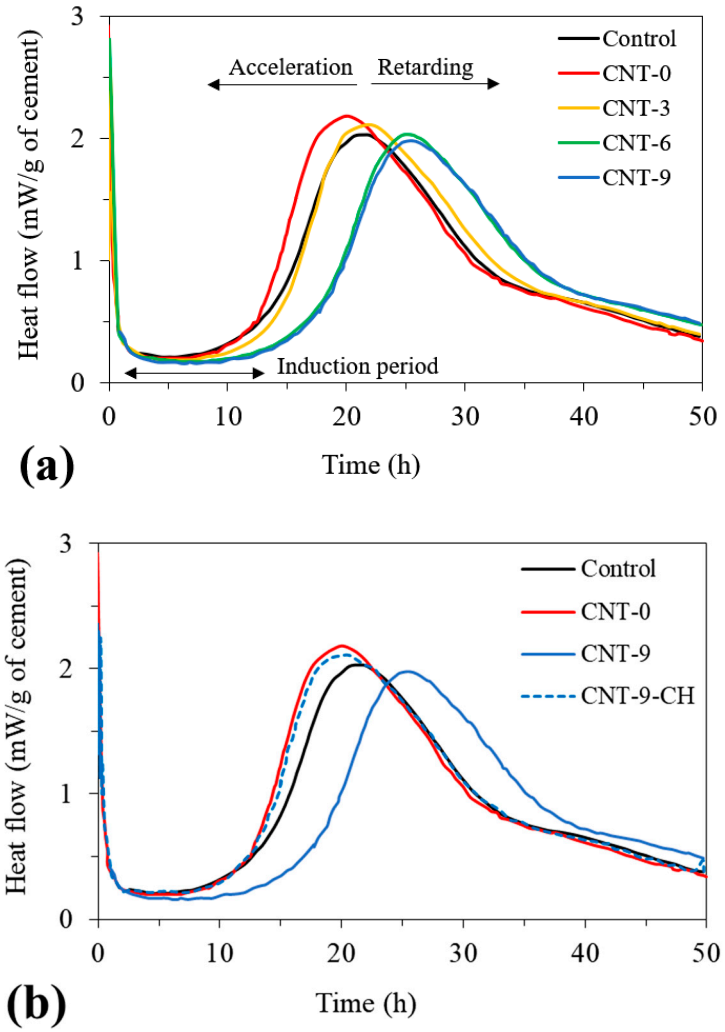

Figure 4. Isothermal calorimetry curves of the cement pates. (**a**) CNT with different exposure times Table 2. SO_4/HNO_3. (**b**) CNT with and without subsequent $Ca(OH)_2$ neutralization.

4. Conclusions

This work investigated the combined functionalization of CNT with H_2SO_4/HNO_3 and $Ca(OH)_2$ for addition in a cementitious matrix. Zeta potential and visual sedimentation indicated that the acid functionalization improved the dispersion and stability of CNT in water. Despite the increase in ID/IG ratio in Raman, SEM showed that H_2SO_4/HNO_3 exposure did not lead to evident damage in the CNT's morphology. However, the increase in the acid exposure time progressively delayed the early-age hydration kinetics of cement paste with the CNT. Further $Ca(OH)_2$ neutralization limited the dispersion improvement promoted by acid treatment but compensated the undesired hydration delay, leading to equivalent cement hydration kinetics to un-treated CNT with improved stability.

Author Contributions: Conceptualization, E.B.; Data curation, P.R.d.M.; Formal analysis, R.F.; Funding acquisition, P.J.P.G. and M.K.; Investigation, E.B. and S.K.; Resources, P.J.P.G. and N.V.; Software, S.K.; Supervision, P.J.P.G.; Writing—original draft, E.B., P.R.d.M., P.J.P.G., R.F., S.K., N.V. and M.K. All authors have read and agreed to the published version of the manuscript.

Funding: The research is partially funded by the Ministry of Science and Higher Education of the Russian Federation as part of World-class Research Center program: Advanced Digital Technologies (contract No. 075-15-2020-934 dated 17 November 2020).

Institutional Review Board Statement: Not applicable.

Informed Consent Statement: Not applicable.

Data Availability Statement: Not applicable.

Acknowledgments: The authors acknowledge CAPES, CNPq and FAPESC from Brazil for the financial support, and LCME-UFSC for the SEM analysis.

Conflicts of Interest: The authors declare no conflict of interest.

References

1. Wang, B.; Han, Y.; Liu, S. Effect of highly dispersed carbon nanotubes on the flexural toughness of cement-based composites. *Constr. Build. Mater.* **2013**, *46*, 8–12. [CrossRef]
2. Klyuev, S.V.; Klyuev, A.V.; Khezhev, T.A.; Pukharenko, Y.V. High-strength fine-grained fiber concrete with combined reinforcement by fiber. *J. Eng. Appl. Sci.* **2018**, *13*, 6407–6412.
3. Pimenov, A.I.; Ibragimov, R.A.; Izotov, V.S. Research on the influence of the carbon nanotubes injection method on cement composite properties. *ZKG Int.* **2015**, *68*, 46–48.
4. Klyuyev, A.; Sopin, D.; Netrebenko, A.; Kazlitin, S. Heavy loaded floors based on fine-grained fiber concrete. *Mag. Civ. Eng.* **2013**, *38*, 7–14. [CrossRef]
5. Tafesse, M.; Kim, H.-K. The role of carbon nanotube on hydration kinetics and shrinkage of cement composite. *Compos. Part B Eng.* **2019**, *169*, 55–64. [CrossRef]
6. Karpov, D. The algorithm of complex diagnostics of technical condition of building structures on thermograms analysis. *Constr. Mater. Prod.* **2020**. [CrossRef]
7. Ibragimov, R.R.; Izotov, V.S. Effect of carbon nanotubes on the structure and properties of cement composites. *Inorg. Mater.* **2015**, *51*, 834–839. [CrossRef]
8. Amran, M.; Fediuk, R.; Vatin, N.; Lee, Y.H.; Murali, G.; Ozbakkaloglu, T.; Klyuev, S.; Alabduljabbar, H. Fibre-Reinforced Foamed Concretes: A Review. *Materials* **2020**, *13*, 4323. [CrossRef]
9. Vaisman, L.; Wagner, H.D.; Marom, G. The role of surfactants in dispersion of carbon nanotubes. *Adv. Colloid Interface Sci.* **2006**, *128–130*, 37–46. [CrossRef]
10. Fediuk, R.S. Mechanical Activation of Construction Binder Materials by Various Mills. In Proceedings of the IOP Conference Series: Materials Science and Engineering, Yurga, Russia, 26–28 November 2015; Volume 125, p. 012019.
11. Petrunin, S.; Vaganov, V.; Reshetniak, V.; Zakrevskaya, L. *Influence of Carbon Nanotubes on the Structure Formation of Cement Matrix*; IOP Publishing: Bristol, UK, 2015; Volume 96, p. 012046.
12. Fediuk, R.; Amran, M.; Mosaberpanah, M.A.; Danish, A.; El-Zeadani, M.; Klyuev, S.; Vatin, N. A Critical Review on the Properties and Applications of Sulfur-Based Concrete. *Materials* **2020**, *13*, 4712. [CrossRef]
13. Pierard, N.; Fonseca, A.; Konya, Z.; Willems, I.; Van Tendeloo, G.; Nagy, J. Production of short carbon nanotubes with open tips by ball milling. *Chem. Phys. Lett.* **2001**, *335*, 1–8. [CrossRef]
14. Liu, F.; Zhang, X.; Cheng, J.; Tu, J.; Kong, F.; Huang, W.; Chen, C. Preparation of short carbon nanotubes by mechanical ball milling and their hydrogen adsorption behavior. *Carbon* **2003**, *41*, 2527–2532. [CrossRef]
15. Nizina, T.; Ponomarev, A.; Balykov, A.; Pankin, N. Fine-grained fibre concretes modified by complexed nanoadditives. *Int. J. Nanotechnol.* **2017**, *14*, 665. [CrossRef]
16. Kharun, M.; Klyuev, S.; Koroteev, D.; Chiadighikaobi, P.C.; Fediuk, R.; Olisov, A.; Vatin, N.; Alfimova, N. Heat Treatment of Basalt Fiber Reinforced Expanded Clay Concrete with Increased Strength for Cast-In-Situ Construction. *Fibers* **2020**, *8*, 67. [CrossRef]
17. Konsta-Gdoutos, M.S.; Metaxa, Z.S.; Shah, S.P. Highly dispersed carbon nanotube reinforced cement based materials. *Cem. Concr. Res.* **2010**, *40*, 1052–1059. [CrossRef]
18. Jung, M.; Lee, Y.-S.; Hong, S.-G.; Moon, J. Carbon nanotubes (CNTs) in ultra-high performance concrete (UHPC): Dispersion, mechanical properties, and electromagnetic interference (EMI) shielding effectiveness (SE). *Cem. Concr. Res.* **2020**, *131*, 106017. [CrossRef]
19. Tolstoy, A.D.; Lesovik, V.S.; Glagolev, E.S.; Krymova, A.I. *Synergetics of Hardening Construction Systems*; IOP Conference Series: Materials Science and Engineering; IOP Publishing: Bristol, UK, 2018; Volume 327, p. 032056.
20. De Azevedo, A.R.; Klyuev, S.; Marvila, M.T.; Vatin, N.; Alfimova, N.; De Lima, T.E.; Fediuk, R.; Olisov, A. Investigation of the Potential Use of Curauá Fiber for Reinforcing Mortars. *Fibers* **2020**, *8*, 69. [CrossRef]
21. Martin, C.; Sandler, J.; Windle, A.; Schwarz, M.-K.; Bauhofer, W.; Schulte, K.; Shaffer, M. Electric field-induced aligned multi-wall carbon nanotube networks in epoxy composites. *Polymer* **2005**, *46*, 877–886. [CrossRef]
22. Klyuev, S.V.; Khezhev, T.; Pukharenko, Y.; Klyuev, A. To the Question of Fiber Reinforcement of Concrete. *Mater. Sci. Forum* **2019**, *945*, 25–29. [CrossRef]
23. Artamonova, O.V.; Slavcheva, G.S.; Shvedova, M.A. Effectiveness of Nanotubular Additives in the Modification of Cement Systems. *Inorg. Mater.* **2020**, *56*, 105–110. [CrossRef]
24. Da Luz, G.; Gleize, P.J.; Batiston, E.R.; Pelisser, F. Effect of pristine and functionalized carbon nanotubes on microstructural, rheological, and mechanical behaviors of metakaolin-based geopolymer. *Cem. Concr. Compos.* **2019**, *104*, 103332. [CrossRef]
25. Khuzin, A.; Ibragimov, R.R. Processes of structure formation and paste matrix hydration with multilayer carbon nanotubes additives. *J. Build. Eng.* **2020**, 102030. [CrossRef]

26. De Lannoy, C.-F.; Soyer, E.; Wiesner, M.R. Optimizing carbon nanotube-reinforced polysulfone ultrafiltration membranes through carboxylic acid functionalization. *J. Membr. Sci.* **2013**, *447*, 395–402. [CrossRef]
27. Ibragimov, R.; Fediuk, R. Improving the early strength of concrete: Effect of mechanochemical activation of the cementitious suspension and using of various superplasticizers. *Constr. Build. Mater.* **2019**, *226*, 839–848. [CrossRef]
28. Stroganov, V.; Sagadeev, E.; Ibragimov, R.R.; Potapova, L. Mechanical activation effect on the biostability of modified cement compositions. *Constr. Build. Mater.* **2020**, *246*, 118506. [CrossRef]
29. Shi, T.; Li, Z.; Guo, J.; Gong, H.; Gu, C. Research progress on CNTs/CNFs-modified cement-based composites—A review. *Constr. Build. Mater.* **2019**, *202*, 290–307. [CrossRef]
30. Fediuk, R.S.; Lesovik, V.S.; Liseitsev, Y.L.; Timokhin, R.A.; Bituyev, A.V.; Zaiakhanov, M.Y.; Mochalov, A.V. Composite binders for concretes with improved shock resistance. *Mag. Civ. Eng.* **2019**, *85*, 3. [CrossRef]
31. Klyuyev, S.; Guryanov, Y. External reinforcing of fiber concrete constructions by carbon fiber tapes. *Mag. Civ. Eng.* **2013**, *36*, 21–26. [CrossRef]
32. Jansen, D.; Goetz-Neunhoeffer, F.; Lothenbach, B.; Neubauer, J. The early hydration of Ordinary Portland Cement (OPC): An approach comparing measured heat flow with calculated heat flow from QXRD. *Cem. Concr. Res.* **2012**, *42*, 134–138. [CrossRef]
33. Khezhev, T.A.; Pukharenko, Y.V.; Khezhev, K.A.; Klyuev, S.V. Fiber gypsum concrete composites with using volcanic tuffsawing waste. *ARPN J. Eng. Appl. Sci.* **2018**, *13*, 2935–2946.
34. Matos, P.R.; Oliveira, J.C.; Medina, T.M.; Magalhães, D.C.; Gleize, P.J.; Schankoski, R.A.; Pilar, R. Use of air-cooled blast furnace slag as supplementary cementitious material for self-compacting concrete production. *Constr. Build. Mater.* **2020**, *262*, 120102. [CrossRef]
35. Scrivener, K.L.; Juilland, P.; Monteiro, P.J. Advances in understanding hydration of Portland cement. *Cem. Concr. Res.* **2015**, *78*, 38–56. [CrossRef]
36. Begich, Y.E.; Klyuev, S.V.; Jos, V.A.; Cherkashin, A.V. Fine-grained concrete with various types of fibers. *Mag. Civ. Eng.* **2020**, *96*, 2. [CrossRef]
37. De Matos, P.R.; Sakata, R.D.; Onghero, L.; Uliano, V.G.; De Brito, J.; Campos, C.E.; Gleize, P.J. Utilization of ceramic tile demolition waste as supplementary cementitious material: An early-age investigation. *J. Build. Eng.* **2021**, *38*, 102187. [CrossRef]
38. Reales, O.A.M.; Pearl, W.C.; Paiva, M.D.M.; Miranda, C.R.; Filho, R.D.T. Effect of a commercial dispersion of multi walled carbon nanotubes on the hydration of an oil well cementing paste. *Front. Struct. Civ. Eng.* **2015**, *10*, 174–179. [CrossRef]
39. Isfahani, F.T.; Li, W.; Redaelli, E. Dispersion of multi-walled carbon nanotubes and its effects on the properties of cement composites. *Cem. Concr. Compos.* **2016**, *74*, 154–163. [CrossRef]
40. Ahmed, H.; Bogas, J.A.; Guedes, M.; Pereira, M.F.C.; Hawreen, A. Dispersion and reinforcement efficiency of carbon nanotubes in cementitious composites. *Mag. Concr. Res.* **2019**, *71*, 408–423. [CrossRef]
41. Associação Brasileira de Normas Técnicas. *Norma Brasileira: NBR 16697-Cimento Portland—Requisitos*; ABNT: Rio de Janeiro, Brazil, 2018. (in Portuguese)
42. Wepasnick, K.A.; Smith, B.A.; Schrote, K.E.; Wilson, H.K.; Diegelmann, S.R.; Fairbrother, D.H. Surface and structural characterization of multi-walled carbon nanotubes following different oxidative treatments. *Carbon* **2011**, *49*, 24–36. [CrossRef]
43. Chen, J.J.; Thomas, J.J.; Taylor, H.F.; Jennings, H.M. Solubility and structure of calcium silicate hydrate. *Cem. Concr. Res.* **2004**, *34*, 1499–1519. [CrossRef]
44. Ding, D.; Wang, J.; Yu, X.; Xiao, G.; Feng, C.; Xu, W.; Bai, B.; Yang, N.; Gao, Y.; Hou, X.; et al. Dispersing of functionalized CNTs in Si–O–C ceramics and electromagnetic wave absorbing and mechanical properties of CNTs/Si–O–C nanocomposites. *Ceram. Int.* **2020**, *46*, 5407–5419. [CrossRef]
45. Cavaliere, P. (Ed.) *Spark Plasma Sintering of Materials: Advances in Processing and Applications*; Springer: Berlin, Germany, 2019.
46. Berodier, E.; Scrivener, K. Understanding the Filler Effect on the Nucleation and Growth of C-S-H. *J. Am. Ceram. Soc.* **2014**, *97*, 3764–3773. [CrossRef]
47. Li, G.Y.; Wang, P.M.; Zhao, X. Mechanical behavior and microstructure of cement composites incorporating surface-treated multi-walled carbon nanotubes. *Carbon* **2005**, *43*, 1239–1245. [CrossRef]
48. Usanova, K.; Barabanshchikov, Y.G. Cold-bonded fly ash aggregate concrete. *Mag. Civ. Eng.* **2020**, *95*, 104–118. [CrossRef]
49. Korsun, V.I.; Vatin, N.; Korsun, A.; Nemova, D. Physical-Mechanical Properties of the Modified Fine-Grained Concrete Subjected to Thermal Effects up to 200 °C. *Appl. Mech. Mater.* **2014**, *633*, 1013–1017. [CrossRef]